THE JOURNAL OF PHYSICAL CHEMISTRY B LETTERS

2005, *109,* 12658−12662
Published on Web 06/14/2005

Single-Molecule Tracking of Sub-millisecond Domain Motion in Calmodulin

Brian D. Slaughter,[†] Ramona J. Bieber-Urbauer,[‡] and Carey K. Johnson*[,†]

Department of Chemistry, 1251 Wescoe Hall Drive, University of Kansas, Lawrence, Kansas 66045-7582, and Department of Chemistry and Department of Biochemistry and Molecular Biology, University of Georgia, Athens, Georgia 30602

Received: April 1, 2005; In Final Form: May 23, 2005

We used single-pair fluorescence resonance energy transfer (spFRET) to track distance changes between domains of fluorescently labeled calmodulin (CaM) on the sub-millisecond time scale. In most cases, CaM remained in the same conformational substate over time periods of up to 1 ms, showing that conformational interchange occurs on a longer time scale. However, in some instances, apparent transitions between conformational substates could be detected. The magnitude of sub-millisecond motion within the dominant conformational substate also revealed fluctuations in distance between domains that were dependent on pH and ionic strength.

Introduction

Calmodulin (CaM) is a small, multidomain, Ca^{2+}-signaling protein which, upon binding four Ca^{2+} ions, binds numerous target proteins with high affinity.[1] We used a CaM mutant with two cysteine residues, CaM-T34C-T110C, labeled at opposing globular domains with the fluorescence resonance energy transfer (FRET) pair Alexa-Fluor 488 and Texas Red (CaM-DA)[2] (Figure 1A, 1cfd[3]) to track the domain motion of CaM on the sub-millisecond time scale by single-pair fluorescence resonance energy transfer (spFRET).[4] Numerous studies have examined the structure of Ca^{2+}-CaM and CaM in the absence of Ca^{2+} (apoCaM).[5−7] However, the roles of structural heterogeneity and conformational dynamics in the interactions of CaM with target proteins are not well understood.

Single-molecule spectroscopy[8−13] and fluorescence correlation spectroscopy (FCS)[14−17] can be used to detect protein dynamics and to sample multiple substates in proteins. We recently applied FCS cross-correlation of the donor and acceptor emission intensity of CaM-DA to reveal Ca^{2+}-dependent motion between lobes of CaM on the time scale of hundreds of microseconds and milliseconds.[18] spFRET analysis of fluorescence bursts in our laboratory revealed that CaM-DA is present in multiple conformational substates, as characterized by the distance between probes at sites 34 and 110: a dominant 30−40 Å conformation, a compact 20−30 Å conformation, and an extended 50−60 Å conformation.[18,19]

The presence of these conformational substates raises the question of the time scale of conformational interchange and how these time scales relate to the interchange of conformational substates. In the current study, single-molecule trajectories were obtained in order to analyze interchange between conformational substates. We found that CaM is unlikely to undergo transitions between conformational substates on the sub-millisecond time scale, but single-molecule distance trajectories revealed rare examples of apparent conformational change. These motions may be crucial to the interaction of CaM with its targets.

Experimental Methods

CaM T34/110C was expressed, purified, fluorescently labeled, and separated following methods described previously.[2,20] Briefly, threonine residues 34 and 110 of chicken CaM (CaM T34/110C) were mutated to cysteines using polymerase chain reaction (PCR). The expression vector of CaM T34/110C was inoculated in *E. coli* and grown in a standard M9 medium. The culture was harvested, and the CaM mutant was purified using a Phenyl Sepharose CL-4B resin. The purified CaM T34/110C was labeled simultaneously with Alexa Fluor 488 maleimide (AF488) as donor (D) and Texas Red maleimide (TR) as acceptor (A). The double-labeled construct (CaM-DA) was separated by reverse phase high-performance liquid chromatography (HPLC) and a C5 Bio Wide Pore column,[2,20] yielding a pure sample of CaM-DA with negligible amounts of CaM-DD and CaM-AA (see Supporting Information in ref 2). The fluorescent lifetimes of CaM-T34C-AF488 and CaM-T110-AF488 are nearly identical (4.13 ns for Ca^{2+}-CaM-T34C-AF488 and 3.88 ns for Ca^{2+}-CaM-T110C-AF488), as are the lifetimes for CaM-T34C-TR and CaM-T110-TR (4.73 ns for Ca^{2+}-CaM-T34C-TR and 4.76 ns for Ca^{2+}-CaM-T110C-TR).[18] The corresponding quantum efficiencies for each dye are also nearly identical for the two possible labeling sites: 0.82 for Ca^{2+}-CaM-T34C-AF488 and 0.78 for Ca^{2+}-CaM-T110C-AF488; 0.61 for Ca^{2+}-CaM-T34C-TR and 0.60 for Ca^{2+}-CaM-T110C-TR. Given that the calculated distance, R, between donor and acceptor depends on the one-sixth power of the quantum yield, differences between distances determined for the two possible FRET pairs, CaM-$D_{34}A_{110}$ and CaM-$D_{110}A_{34}$, are expected to be negligible.

Buffer conditions for the Ca^{2+} experiments consisted of 10 mM HEPES, pH 7.4, 0.1 M KCl, 1 mM $MgCl_2$, and 0.1 mM $CaCl_2$ (buffer K). The same buffer but with 300 μM EGTA

* Corresponding author. E-mail: ckjohnson@ku.edu. Phone: 785-864-4219. Fax: 785-864-5396.
[†] University of Kansas.
[‡] University of Georgia.

10.1021/jp051666o CCC: $30.25

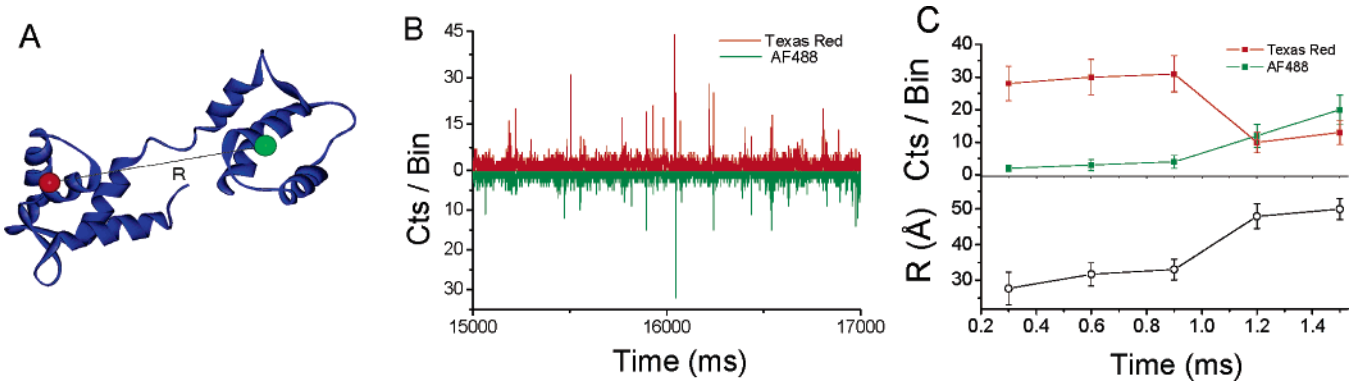

Figure 1. (A) Solution structure of apoCaM (1cfd) illustrating the sites of attachment of AF488 (green) and Texas Red (red). spFRET measurements yield the distance, *R*, between probes. (B) Fluorescence data in 300 μs time bins. Bursts of fluorescence are due to single-CaM-DA molecules traversing the focal region of the microscope. (C) Example of a single-molecule burst showing counts in donor and acceptor channels. The FRET efficiency and distance between probes were found from relative donor and acceptor counts.

was used for low-Ca^{2+} measurements, resulting in a free Ca^{2+} level of ~150 nM. The free Ca^{2+} level was verified using the Ca^{2+} indicators calcium green-1 and 5,5′-dibromo-BABTA and standard Ca^{2+} buffers at identical Mg^{2+}, pH, and ionic strength (Molecular Probes, Eugene, OR). For low-Ca^{2+} studies at low ionic strength, CaM-DA was dialyzed against 10 mM HEPES, 0.1 mM $CaCl_2$, pH 7.4, in the presence of 300 μM EGTA to remove any residual $MgCl_2$ and KCl.

Single-molecule measurements of freely diffusing CaM-DA were made with an inverted fluorescence microscope (Nikon TE2000) as described previously.[18] The 488 nm line of an Ar^+ laser (Coherent-Innova) was directed into the back of the fluorescence microscope and reflected with a dichroic mirror (Q505LP, Chroma Technologies) onto a 1.3 NA, 100× oil-immersion objective (SuperFluor). After collection by the objective, the emission passed through the same dichroic mirror and out the side port of the microscope. A dichroic filter (565DCLP, Chroma Technologies) was used to separate the donor and acceptor fluorescence emission. Band-pass filters in front of the donor (HQ525/50M, Chroma Technologies) and acceptor (HQ620/75M, Chroma Technologies) channel detectors were used for further discrimination in the fluorescence wavelength. Single-photon counting avalanche photodiodes (SPCM-ARQ-14, Perkin-Elmer) counted the fluorescence photons. The excitation power at the entrance of the objective was 45 μW.

Results and Discussion

Emission from Freely Diffusing CaM-DA. A drop of CaM-DA with a concentration of approximately 100 pM was placed on a microscope slide above the objective. The beam was focused at a minimum 20 μM above the surface. As freely diffusing molecules drifted through the focal region, emission was collected in donor and acceptor channels in 300 μs time bins (Figure 1B). In the picomolar concentration regime, the vast majority of bins (~99%) corresponded to times when no molecule was in the focal region and thus possessed low background counts only, on the order of 1 to 2 counts per bin. Cutoff parameters were implemented to determine when a molecule is present in the focal volume. For data analysis in the present experiment, only bins were included that contained a donor or an acceptor count level that was larger than 6 times the standard deviation of the background signal in the respective channel, or a sum of donor and acceptor counts that was 6 times above the sum of the donor and acceptor background level. One percent of all bins exceeded these cutoff levels. For a set of data, average bleedthrough from the donor to acceptor channel (estimated to be 10%) was subtracted from the acceptor channel. It was required that acceptor counts be above background after the subtraction of donor bleedthrough in order to avoid the inclusion of bins that may be biased toward low FRET efficiency due to acceptor photobleaching. Cutoffs are necessary to ensure the inclusion of only bins with high signal to background. The exact value of these cutoff thresholds is necessarily arbitrary in nature depending on the desired discrimination against background. The choice of cutoff parameters has been discussed in greater detail in a previous publication.[18]

Once it was determined that a bin corresponded to a time period where a CaM-DA molecule was in the focal region, the distance between fluorescent probes was determined from

$$R = \left(\frac{I_d}{c(I_a - bI_d)}\right)^{1/6} R_0 \qquad (1)$$

where I_a and I_d are acceptor and donor fluorescent counts, c is a factor to correct for the relative detection efficiency of the donor and acceptor channels,[18] and b subtracts the average bleedthrough from the donor channel to the acceptor channel. The value of b (typically 0.10) was determined from the ratio of CaM-AF488 emission in donor and acceptor channels. A single value of b is used with the assumption that the emission spectrum of CaM-AF488 is uniform. The single-exponential fluorescence decay of singly labeled CaM-AF488 suggests that the dye exists in a homogeneous environment and thus that spectral jumps are unlikely.[18,19] The value of c was 1.2, determined by comparison of an ensemble FRET measurement on the microscope with the FRET efficiency measured from a fluorimeter scan. (We have, however, not included a correction factor to account for the relative quantum yields of donor and acceptor, estimated to be ~0.95 in the calculated distance.) R_0 is the Förster distance, or distance of 50% energy transfer between donor and acceptor. For AF488 and TR, an R_0 value of 46.5 Å was calculated.[18,19] An example of a single-molecule burst and the corresponding calculated R values is shown in Figure 1C. Transit times for single molecules ranged up to a few milliseconds in the present setup. During a single-molecule burst, there were some bins with low count levels in both donor and acceptor channels. In the analysis of a whole single-molecule burst, the bins with low count levels led to a large uncertainty in distance, which could bias analysis. Therefore, in the analysis described here, only the changes in distance between successive high-signal bins were included, minimizing uncertainty due to Poisson counting noise.

Comparison of *R* in Successive Bins. Inspection of high-signal bins in time order revealed sequences of successive, high-

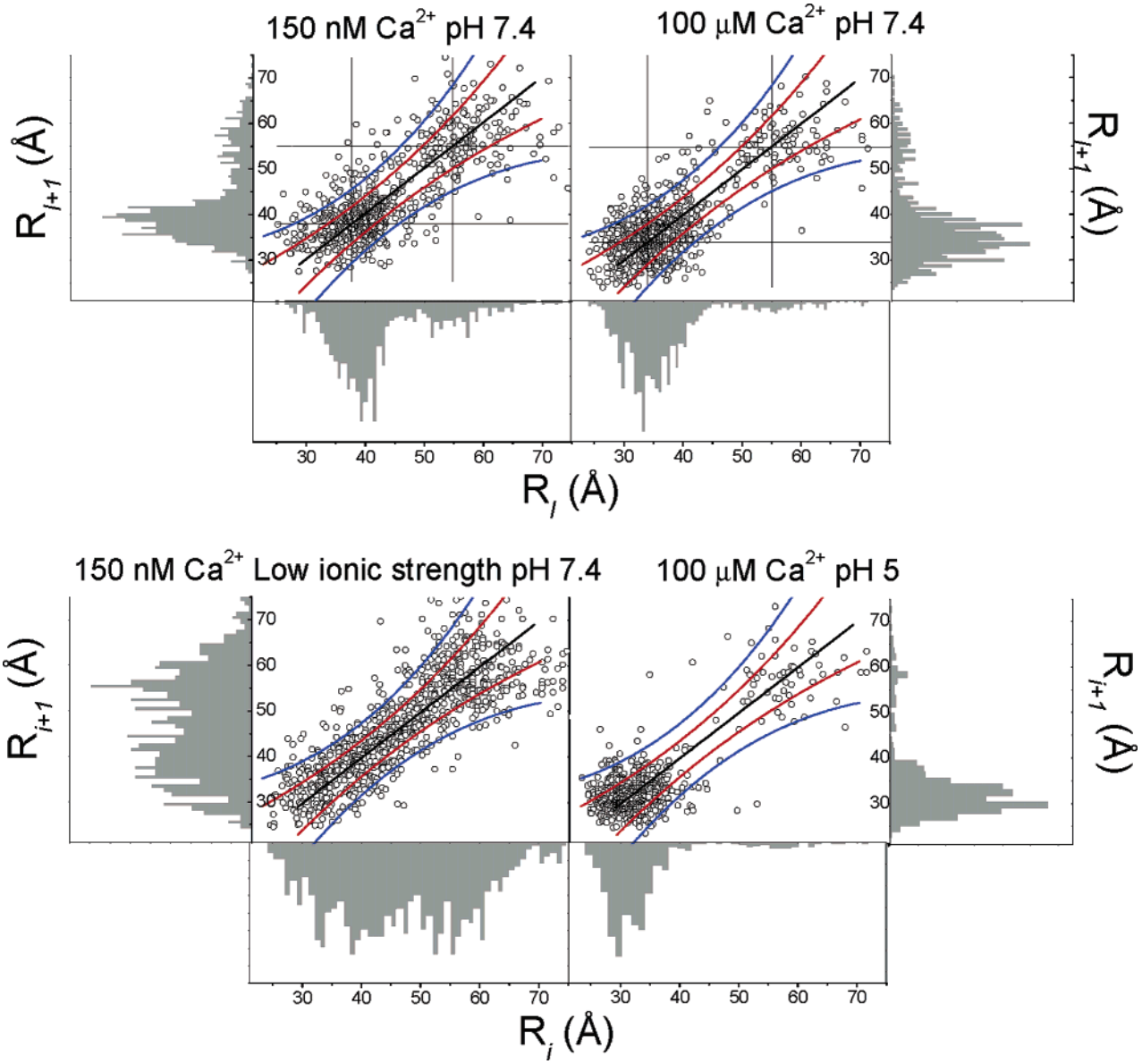

Figure 2. *R* values between successive high-signal bins, where R_i represents a bin with fluorescence counts above the selection criteria and R_{i+1} represents the bin immediately following. Data were included only if fluorescence counts were sufficient to have confidence in a calculated distance for a bin (i) and the bin immediately following ($i + 1$). The red and blue curves represent the Poisson uncertainty in *R* at the 68th and 95th percentile based on average donor and acceptor counts at each *R* value. The R_i and R_{i+1} distance distributions are shown as projections along each axis. A Wilcoxon test of the R_i and R_{i+1} distributions showed that differences in the R_i and R_{i+1} distributions are insignificant, with significance levels for the null hypothesis of $p = 0.64$ for apoCaM, 0.18 for Ca^{2+}-CaM, 0.90 for CaM at low ionic strength, and 0.60 for CaM at pH 5.

signal bins. At the picomolar concentration regime, it is extremely unlikely that two CaM-DA molecules reside in the focal volume simultaneously. On average, there was a molecule in the focal volume approximately 1.0% of the time, and therefore, only 0.01% of the time were there two. Thus, a change in the ratio of donor and acceptor counts between successive high-signal bins can be related to a distance change between lobes of CaM. If fluorescence counts were sufficient to have confidence in a calculated distance for a bin (i) and the bin immediately following ($i + 1$), then the relation between the distance between lobes averaged over successive time periods was known and was represented by a single data point in Figure 2. Points are plotted for cases where the fluorescence signal was sufficient to determine the distance, *R*, between donor and acceptor for two consecutive high-signal bins. The initial *R*, R_i, is plotted on the *x*-axis, with R_{i+1} on the *y*-axis. The distributions of all initial *R* values (i) and all final *R* values ($i + 1$) are shown as projections along each axis. The similarity of the distributions of initial and final *R* values verified that acceptor photobleaching did not significantly influence the measured distributions. If acceptor photobleaching were significant during the observation of single-CaM-DA molecules, we would expect to find $\langle R_{i+1} \rangle$ greater than $\langle R_i \rangle$. However, we found $\langle R_i \rangle \approx \langle R_{i+1} \rangle$: 37.2 ± 0.3 Å versus 37.4 ± 0.3 Å for Ca^{2+}-CaM-DA, 42.7 ± 0.3 Å versus 42.8 ± 0.3 Å for apo-CaM-DA, 31.4 ± 0.4 Å versus 31.5 ± 0.4 Å for pH 5.0 Ca^{2+}-CaM-DA, and 46.9 ± 0.4 Å versus 46.9 ± 0.4 Å for apo-CaM-DA at reduced ionic strength.

Figure 2 plots the distance between lobes of CaM for successive 300 μs bins for CaM at low Ca^{2+}, where it is likely that each CaM molecule has zero to one Ca^{2+} bound, and at saturating Ca^{2+}, where each CaM molecule has four Ca^{2+} ions bound. Data for reduced pH and reduced ionic strength are also shown. Most of the points in Figure 2 lie in two ranges centered at distances around 34 and 55 Å for Ca^{2+}-CaM, and 38 and 55 Å for apoCaM, corresponding to the two largest peaks in the distance distributions.[18,19] The highest density of points falls

TABLE 1: Experimental, $\langle \Delta R^2 \rangle^{1/2}_{exptl}$, rms Fluctuations between Lobes of CaM between Successive High-Signal 300 μs Bins, Compared to rms Fluctuations for Model Data with Poisson Noise, $\langle \Delta R^2 \rangle^{1/2}_{Poi}$, Based on Average Donor and Acceptor Count Rates

	$\langle \Delta R^2 \rangle^{1/2}_{exptl}$ (Å)		$\langle \Delta R^2 \rangle^{1/2}_{Poi}$ (Å)	
	R_i < 47 Å	R_i > 47 Å	R_i < 47 Å	R_i > 47 Å
Ca^{2+}-CaM	5.3 ± 0.2	7.7 ± 0.8	4.5 ± 0.2	7.1 ± 0.2
apoCaM	5.2 ± 0.2	7.7 ± 0.5	4.2 ± 0.1	6.9 ± 0.2
apo-low ionic strength	5.8 ± 0.3	7.8 ± 0.4	4.5 ± 0.1	6.8 ± 0.2
pH 5.0 Ca^{2+}-CaM	4.5 ± 0.2		4.4 ± 0.2	

into a circular region consistent with the existence of well-defined conformational substates on this time scale. This result shows that if CaM exists in one conformation for a given time bin, it is likely that it will remain in this conformation over the next 300 μs time period, indicating that conformational interchange occurs on a time scale slower than 300 μs. An indication of the fraction of conformational changing events is provided by the probability of a transition from the compact to the extended conformation or vice versa, defined here as a transition from R below 48 Å to above 48 Å or vice versa with a ΔR value of at least 10 Å. This probability is 3.3% for apoCaM, 1.7% for Ca^{2+}-CaM, 2.9% for low CaM at ionic strength, and 1.0% for CaM at pH 5.

At a reduced pH, the higher concentration of points around R = 32 Å indicates an increased population of compact conformations of CaM, as reported previously.[19] There are few changes in distance at reduced pH that are outside of the variation in R expected from Poisson counting noise. In contrast, at low ionic strength and low Ca^{2+}, CaM is able to sample a wider range of conformations, with R values that are not restricted to the two regions that are heavily populated at physiological ionic strength.

Root Mean Square (rms) Analysis. The majority of R values correspond to distances that belong to either the 30−40 Å conformation or the 50−60 Å conformation. Therefore, it was possible to calculate the rms ΔR within each conformational substate, where $\Delta R = R_{i+1} - R_i$. The rms ΔR allows for direct comparison of the amplitude of motion within the conformational substates and the effect of solution conditions on distance fluctuations between lobes of CaM. The rms ΔR expected due to Poisson noise within each group was modeled on the basis of the average single-molecule donor and acceptor count rates within each of the subpopulations of CaM. Experimental rms ΔR values exceeded that expected by Poisson counting noise. Statistically, the rms Poisson counting noise was greater for the extended conformation due to significantly lower acceptor count rates. The rms ΔR expected from Poisson noise is similar in the current experiment regardless of Ca^{2+} level, pH, or ionic strength. However, the experimental rms ΔR values depend on solution conditions, emphasizing the presence of solution-dependent sub-millisecond dynamics of CaM. These results are summarized in Table 1.

Fluctuations in the more compact conformation were most pronounced for CaM at low Ca^{2+} and low ionic strength. In contrast, for Ca^{2+}-CaM at low pH, the rms ΔR values were consistent with the values expected from Poisson noise alone. Previous studies in our laboratory of the reorientational motion

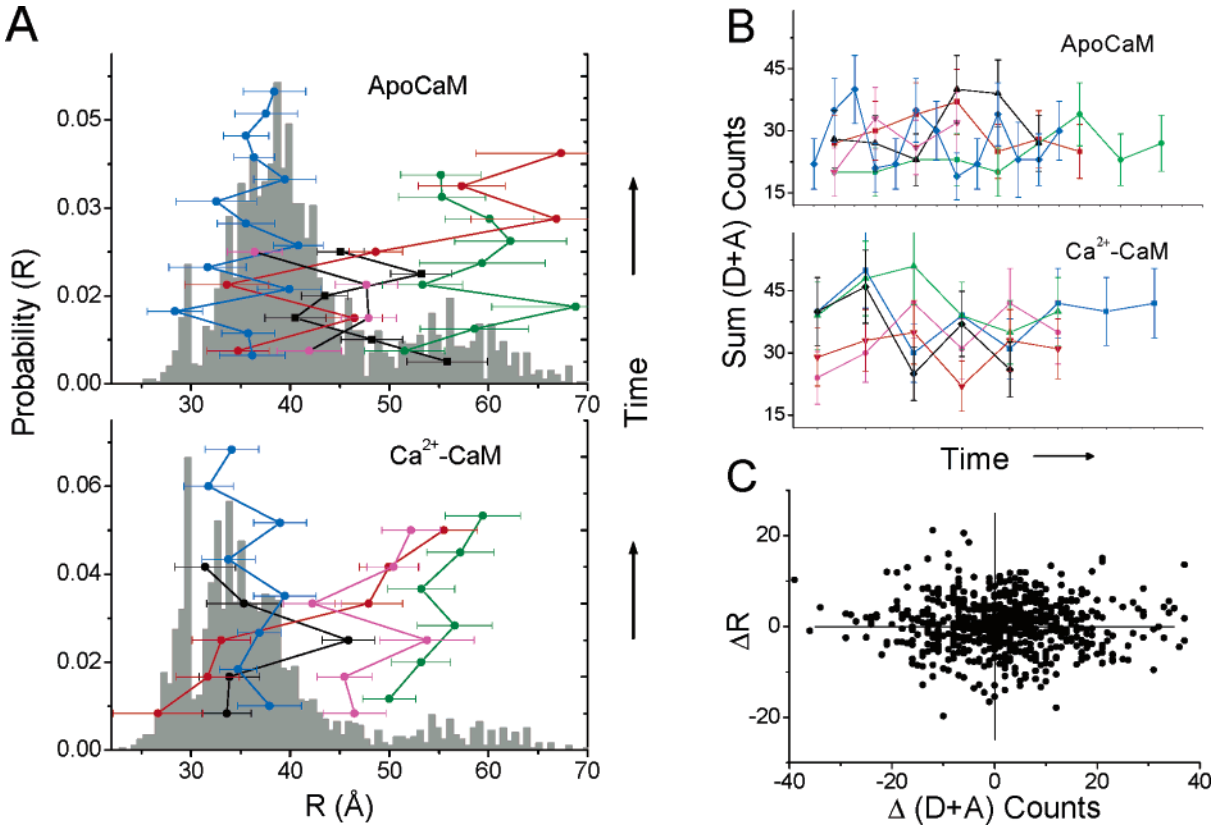

Figure 3. (A) Single-molecule trajectories representing examples of motion within conformational substates or transitions between substates. The single-molecule distributions of spFRET distances at high and low Ca^{2+} are also shown (gray histograms). The y-axis labels give the probability of populating a bin of a particular R value (x-axis). (B) Count totals for the trajectories in part A showing that conformational exchange is not associated with large total intensity changes. (C) Δ(D + A) counts for each data point in Figure 2 (apoCaM combined with Ca^{2+}-CaM) plotted vs ΔR. No correlation was found between ΔR and Δ(D + A) counts, providing evidence that conformational fluctuations are not due to the appearance or removal of a second molecule in the focal volume. The correlation coefficient for the absolute value of ΔR vs the absolute value of Δ(D + A) is 0.016, with an observed significance level of p = 0.68 for the null hypothesis, indicating no correlation.

of the fluorescent probes[18,19] showed extensive free reorientational motion of AF488 on the time scale of hundreds of picoseconds, ensuring minimal uncertainty in R due to incomplete orientational averaging. Also, dye reorientation as characterized by time-resolved anisotropy measurements was largely unchanged regardless of solution conditions such as pH and ionic strength.[19] The larger rms ΔR values for the compact conformation in the other cases therefore indicate the presence of intramolecular conformational fluctuations and demonstrate that changes in pH and ionic strength do not merely result in a change in the conformational substates of CaM[19] but they also result in changes in dynamic motion on the sub-millisecond time scale. We speculate that the dynamic fluctuations may be sensitive to electrostatic interactions involving acidic amino acids in the central linker of CaM.[19]

Domain Tracking of Single CaM Molecules. For molecules that persist in the focal volume for an extended period, it is possible to track the distance between domains for multiple time bins. A number of single-molecule distance trajectories were obtained where several successive bins had count levels above the cutoff criteria. A subset is shown in Figure 3A. The vast majority of single-molecule trajectories showed motion within a single sub-conformation of CaM, again indicating that interchange among sub-conformations typically occurred on a time scale slower than ~1 ms. In Figure 3, the blue and green trajectories show examples of motion within a sub-conformation, while the black trajectories show examples where CaM sampled both major conformations during the observation time. Perhaps the most interesting examples of observed distance trajectories are shown in red, where CaM was present in one conformation and then crossed to a different substate and remained there during the observation time.

We considered the possibility that the presence of two CaM-DA molecules in the focal volume at the same time might lead to apparent changes in conformation. Figure 3B shows the total (D + A) counts for the single-molecule trajectories in Figure 3A. The entry of a second molecule in the focal volume might be expected to cause a total intensity change. However, there is no apparent correlation between the total intensity and conformational fluctuations. To verify that there is no correlation between total intensity and ΔR, we plotted the change in R versus the change in total counts (D + A) for each R_i, R_{i+1} pair (Figure 3C). The absence of correlation in this plot demonstrates that the conformational changes observed are not the result of the addition or subtraction of a CaM-DA molecule to the focal volume.

The possibility also exists that acceptor photoblinking during a time bin could present the appearance of a transition from the more compact to the more extended conformation. We cannot exclude blinking as a possible cause of transitions that appear to occur for one bin and then return. However, it is unlikely that these apparently rare photoblinking events would occur in consecutive time bins. Thus, trajectories that remain at R values >50 Å for several consecutive time bins, such as those in green or red in Figure 3A, are unlikely to have resulted from blinking. Furthermore, transitions to apparent intermediate distances are almost entirely absent at pH 5 (see Figure 2), conditions where the spectroscopic properties of the acceptor (lifetime, quantum yield, and anisotropy) are unchanged compared to pH 7.4 but the conformations of CaM are altered, suggesting that the difference results from the dynamics of CaM rather than photophysics. Similarly, an analysis of the ΔR distribution shown in Figure 3C indicates that acceptor photobleaching, which could cause a sudden decrease in FRET efficiency, does not contribute to the observed transitions. For example, the number of transitions with $\Delta R > 15$ Å is nearly the same (5 out of 657) as the number of transitions with $\Delta R < -15$ Å (4 out of 657).

Conclusions

Using spFRET, fluctuations in distance between the N- and C-terminal domains of CaM were monitored. The major conclusion of this paper is that interchange of the conformational substates of CaM is rare on the microsecond time scale. Analysis of changes in R between successive time bins shows a high probability of CaM remaining in the same conformational substate. Occasionally, jumps in distance between lobes of CaM were observed that are consistent with CaM sampling multiple conformational substates. On the basis of the likelihood of observing these jumps relative to the average transit time of freely diffusing CaM on the single-molecule microscope, it is likely that exchange among the conformational substates of CaM occurs on the millisecond time scale. rms ΔR analysis also revealed a dependence of the magnitude of sub-millisecond domain motion in CaM on pH and ionic strength. This motion indicates distance fluctuations within conformational substates that are reduced at pH 5.0 relative to physiological pH but increased in magnitude for apoCaM at reduced ionic strength. spFRET thus has revealed that the solution conditions (ionic strength and pH) affect not only the amplitudes of the conformational substates of CaM[19] but also the sub-millisecond dynamics.

Acknowledgment. We thank Dr. Jean Johnson for suggesting and running the statistical significance tests. We acknowledge support for this research from NIH R01 GM58715. B.D.S. acknowledges support from the Dynamic Aspects of Chemical Biology Training Grant (NIH 5 T32 GM08545-09).

References and Notes

(1) Chin, D.; Means, A. R. *Trends Cell Biol.* **2000**, *10*, 322−328.
(2) Allen, M. W.; Urbauer, R. J. B.; Johnson, C. K. *Anal. Chem.* **2004**, *76*, 3630−3637.
(3) Kuboniwa, H.; Tjandra, N.; Grzesiek, S.; Ren, H.; Klee, C. B.; Bax, A. *Nat. Struct. Biol.* **1995**, *2*, 768−776.
(4) Ha, T.; Enderle, T.; Ogletree, D. F.; Chemla, D. S.; Selvin, P. R.; Weiss, S. *Proc. Natl. Acad. Sci. U.S.A.* **1996**, *93*, 6264−6268.
(5) Crivici, A.; Ikura, M. *Annu. Rev. Biophys. Biomol. Struct.* **1995**, *24*, 85−116.
(6) Yamniuk, A. P.; Vogel, H. J. *Mol. Biotechnol.* **2004**, *27*, 33−58.
(7) Vetter, S. W.; Leclerc, E. *Eur. J. Biochem.* **2003**, *270*, 404−414.
(8) Xie, X. S.; Trautman, J. K. *Annu. Rev. Phys. Chem.* **1998**, *49*, 441−480.
(9) Moerner, W. E.; Orrit, M. *Science* **1999**, *283*, 1670−1676.
(10) Brasselet, S.; Peterman, E. J. G.; Moerner, W. E. *J. Phys. Chem. B* **2000**, *104*, 3676−3682.
(11) Schuler, B.; Lipman, E. A.; Eaton, W. A. *Nature* **2002**, *419*, 743−747.
(12) Tan, X.; Hu, D.; Squier, T. C.; Lu, H. P. *Appl. Phys. Lett.* **2004**, *85*, 2420−2422.
(13) Sabanayagam, C. R.; Eid, J. S.; Meller, A. *J. Chem. Phys.* **2005**, *122*, 061103.
(14) Magde, D.; Elson, E. L.; Webb, W. W. *Biopolymers* **1974**, *13*, 29−61.
(15) Muller, J. D.; Chen, Y.; Gratton, E. *Methods Enzymol.* **2003**, *361*, 69−92.
(16) Bismuto, E.; Gratton, E.; Lamb, D. C. *Biophys. J.* **2001**, *81*, 3510−3521.
(17) Chattopadhyay, K.; Saffarian, S.; Elson, E. L.; Frieden, C. *Proc. Natl. Acad. Sci. U.S.A.* **2002**, *99*, 14171−14176.
(18) Slaughter, B. D.; Allen, M. W.; Unruh, J. R.; Urbauer, R. J. B.; Johnson, C. K. *J. Phys. Chem. B* **2004**, *108*, 10388−10397.
(19) Slaughter, B. D.; Unruh, J. R.; Allen, M. W.; Bieber Urbauer, R. J.; Johnson, C. K. *Biochemistry* **2005**, *44*, 3694−3707.
(20) Allen, M. W.; Urbauer, R. J. B.; Zaidi, A.; Williams, T. D.; Urbauer, J. L.; Johnson, C. K. *Anal. Biochem.* **2004**, *325*, 273−284.